ORIENTATION OF SPIN-LABELED MYOSIN HEADS IN GLYCERINATED MUSCLE FIBERS

DAVID D. THOMAS, *Department of Biochemistry, University of Minnesota Medical School, Minneapolis, Minnesota 55455*
ROGER COOKE, *Department of Biochemistry and Biophysics and the Cardiovascular Research Institute, University of California, San Francisco, California 94143 U.S.A.*

ABSTRACT We have used electron paramagnetic resonance (EPR) spectra to study spin labels selectively and rigidly attached to myosin heads in glycerinated rabbit psoas muscle fibers. Because the angle between the magnetic field and the principal axis of the probe determines the position of the EPR absorption line, spectra from labeled fibers oriented parallel to the magnetic field yielded directly the distribution of spin label orientations relative to the fiber axis. Two spin labels, having reactivities resembling iodoacetamide (IASL) and maleimide (MSL), were used. In rigor fibers with complete filament overlap, both labels displayed a narrow angular distribution, full width at half maximum ~15°, centered at angles of 68° (IASL) and 82° (MSL). Myosin subfragments (heavy meromyosin and subfragment-1) were labeled and allowed to diffuse into fibers. The resulting spectra showed the same sharp angular distribution that was found for the labeled fibers. Thus it appears that virtually all myosin heads in a rigor fiber have the same orientation relative to the fiber axis, and this orientation is determined by the actomyosin bond. Experiments with stretched fibers indicated that the spin labels on the fraction of heads not interacting with actin filaments had a broad angular distribution. Addition of ATP to unstretched fibers under relaxing conditions produced orientational disorder, resulting in a spectrum almost indistinguishable from that of an isotropic distribution of probes. Addition of either an ATP analog (AMPPNP) or pyrophosphate produced partial disorder. That is, a fraction of the probes remained sharply oriented as in rigor while a second fraction was in a disordered distribution similar to that of relaxed fibers.

INTRODUCTION

Force is generated during muscle contraction by two proteins, actin and myosin, in the presence of ATP. The ATPase sites of myosin reside in two globular heads that project radially from the thick filaments. These heads interact with the actin of the thin filaments, forming crossbridges between the two filaments. A number of studies have suggested that the orientation of the myosin head relative to the actin filament changes during the contraction cycle. In electron micrographs of rigor muscle, the heads appear to bind to actin at an angle of ~45°, while in relaxed muscle they appear to be perpendicular to the actin filament (Reedy et al., 1965; Reedy, 1967 and 1968). The myosin heads have been shown to be attached to the tail portion of the molecule by a flexible region which permits free rotation of the heads (Mendelson et al., 1973; Thomas et al., 1975). These studies have been used to support models in which the orientation and rotational motion of the myosin head plays a central role in the

mechanism of contraction (H. Huxley, 1969; A. Huxley and Simmons, 1971; reviewed by Tregear and Marston, 1979) and thus measurements of orientation are of great importance.

Several methods have been used to study myosin head orientation in muscle fibers. As mentioned above, electron micrographs provide a direct visualization. However, this method suffers from several drawbacks, including uncertainties in the detection of unattached heads in rigor muscle and limitations on measurements in dynamic situations such as relaxed or contracting muscle. Low-angle x-ray diffraction has provided considerable information on the structure of the filaments and the filament array. However, there is insufficient information in the diffraction patterns to uniquely determine the orientation of the heads, and results have been limited to showing that some models are consistent with the data. Intrinsic tryptophan fluorescence can indicate changes in orientation, but the large number of chromophores involved prevents the determination of absolute configurations (Aronson and Morales, 1969; dos Redemios et al., 1972). The polarization of the fluorescence of dyes attached to the myosin head has also been used to study orientation (Nihei et al., 1974; Borejdo and Putnam, 1977). The disadvantage of this method is that one only obtains three independent numbers from a measurement, which makes it difficult to determine the distribution of head orientations when more than one type of site has been labeled, or when more than one probe orientation is present (Tregear and Mendelson, 1975).

The use of spin labels provides several advantages over the other methods listed above. The electron paramagnetic resonance (EPR) spectrum of a nitroxide radical has orientational resolution. That is, probes with different orientations relative to the applied magnetic field absorb at different positions in the spectrum. Therefore, one can use this spectrum to determine directly the orientation distribution of a population of spin labels. In addition, the application of saturation transfer EPR allows one to obtain information on probe motion on a time scale of interest (Thomas et al., 1975; Thomas et al., 1976). Thus spin labels can provide an excellent monitor of myosin head orientation and rotation. Thomas et al. (1980) have recently succeeded in spin-labeling myosin heads selectively in myofibrils, obtaining a preparation with nearly normal ATPase activity in which the spin labels are rigidly attached to the myosin head framework, thus permitting measurements of head rotational motions by saturation transfer EPR.

In the present study, we have used the above labeling method to label myosin heads selectively (apparently at a single SH group) in glycerinated fibers. By recording conventional EPR spectra from fibers that are uniformly oriented relative to the applied magnetic field, we have determined directly the distribution of probe orientation relative to the fiber axis. We report here the results of these measurements, as affected by ATP, ATP analogues, and stretching fibers beyond rest length.

THEORY

The sensitivity of nitroxide EPR spectra to orientation is revealed in the spin Hamiltonian:

$$\mathcal{H} = \beta \underset{\sim}{S} \cdot \underset{\sim}{g} \cdot \underset{\sim}{H} + \bar{g}\beta \underset{\sim}{S} \cdot \underset{\sim}{T} \cdot \underset{\sim}{I}, \tag{1}$$

where β is the Bohr magneton and $\bar{g}$ is the mean g value. The elements of the $\underset{\sim}{g}$ tensor (describing the Zeeman interaction that couples the electron spin $\underset{\sim}{S}$ and the applied magnetic field $\underset{\sim}{H}$) and $\underset{\sim}{T}$ tensor (describing the hyperfine interaction that couples $\underset{\sim}{S}$ with the nuclear

spin $\underline{I}$) depend on the orientation of the molecular axes with respect to $\underline{H}$. To a good approximation for nitroxide spin labels, these two tensors have axial symmetry, so that the magnetic interactions depend only on $\cos^2\theta$, where θ is the angle between the applied field $\underline{H}$ and the principal magnetic axis of the spin label ($\hat{z}$).

In this case of axial symmetry, the observed resonance magnetic field position is given by

$$H_{res}(\theta, m_I) = H_{res}(0, 0)\left[1 - \frac{\Delta g}{\bar{g}}\sin^2\theta\right] - m_I(T_\parallel^2\cos^2\theta + T_\perp^2\sin^2\theta)^{1/2} \qquad (2)$$

(McCalley et al., 1972), where m_I is the nitrogen nuclear spin quantum number (-1, 0, or $+1$), $g_\parallel$ and $g_\perp$ are the g values when $\theta = 0°$ and 90°, $\Delta g = g_\parallel - g_\perp$, and $T_\parallel$ and $T_\perp$ are the T values when $\theta = 0°$ and 90°.

Fig. 1 shows simulated EPR spectra that would result from a uniformly oriented sample (e.g., a single crystal) having an axially symmetric Hamiltonian. The derivative of absorption is plotted against H_{res}. Note that spectra corresponding to different values of θ are sharply resolved, so that spectra like these could be used to determine θ with an accuracy of one or two degrees. Because there is virtually a one-to-one correspondence between θ and H_{res} for a fixed value of m_I, the EPR spectrum can be used to determine the distribution of θ values relative to the magnetic field, in the case of nonuniform orientation.

In the present study, EPR spectra are recorded from oriented bundles of muscle fibers, and

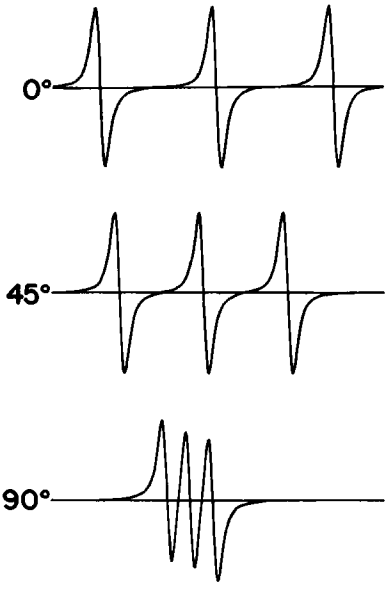

FIGURE 1 Simulated single-crystal EPR spectra. The principal axes of an ensemble of immobilized nitroxide spin-labels are uniformly oriented at an angle θ relative to the applied magnetic field. The anisotropic magnetic interactions (characterized by the g and T tensors) are axially symmetric, with $T_\parallel$ = 35 G, $T_\perp$ = 7 G, $g_\parallel$ = 2.007, Δg = 0.005 (see Eq. 2). The line positions are given by Eq. 2, and the line shapes are derivatives of the Lorentzian $T_2/(1 + \gamma^2 H_{rel}^2 T_2^2)$, where T_2 is the spin-spin relaxation time (2.4×10^{-8} s) (McCalley et al. 1972), γ is the gyromagnetic ratio, and H_{rel} is given by Eq. 2. In these and the following spectra the derivative of absorption is plotted as a function of the magnetic field of the spectrometer, and the width of the baseline is 100 G.

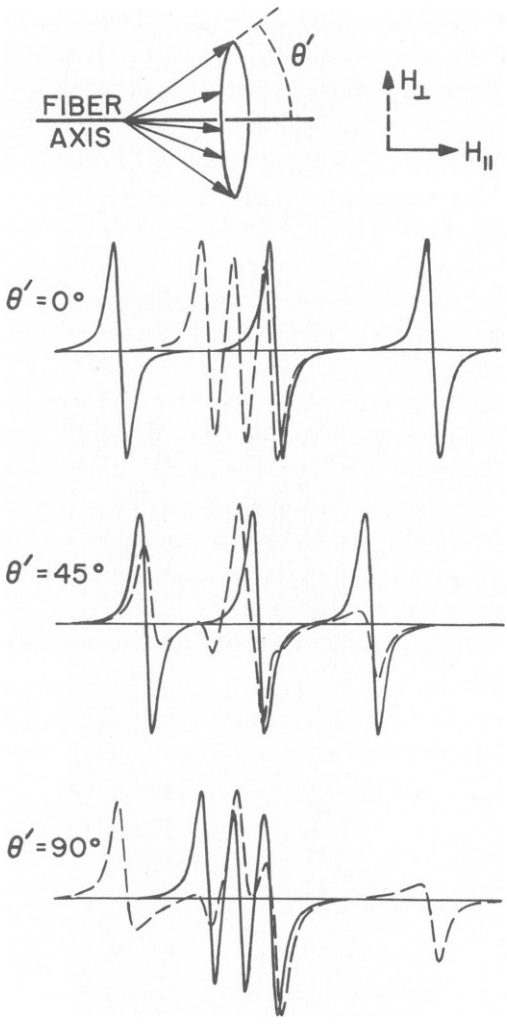

FIGURE 2 Simulated EPR spectra for spin labels uniformly oriented relative to the axes of uniformly oriented muscle fibers. Arrows indicate the orientations of the spin-label's principal axes, which describe the surface of a cone about the fiber axis. The unique angle between the fiber axis and the spin-labels' principal axes is θ', and the angle between the magnetic field and the fiber axis is $\psi = 0°$ ($H_\parallel$, solid curves) or $\psi = 90°$ ($H_\perp$, dashed curves). These spectra were produced by summing single $-\theta'$ spectra (as in Fig. 1) over values of $\varnothing'$ (the azimuthal angle of the label axis) from 0° to 90°, using Eq. 3 to determine θ.

we use these spectra to determine the orientation distribution of spin labels relative to the fiber axes. The distribution of θ values in such a system is determined by the values of θ', where θ' is the angle between the fiber axis and the spin label's principal axis, and ψ, where ψ is the angle between the fiber axis and the magnetic field (see Fig. 2):

$$\cos\theta = \cos\theta'\cos\psi - \sin\theta'\sin\psi\cos\phi'. \tag{3}$$

ϕ', the aximuthal angle of the label axis in the fiber coordinate system, is randomly varied by rotation about the fiber axis.

Fig. 2 shows simulated EPR spectra from spin labels uniformly oriented relative to the fiber axis. The solid curves correspond to $\psi = 0°$, i.e., the fiber axis is parallel to the magnetic field. Under these conditions, $\theta = \theta'$ (see Eq. 3), so the spectra are the same as the single crystal spectra of Fig. 1. The dashed curves correspond to $\psi = 90°$; i.e., the fiber axis is perpendicular to the magnetic field. Then $\cos\theta = -\sin\theta\cos\phi'$ (see Eq. 3), so the variation of ϕ' by rotation about the fiber axis creates a heterogeneous distribution of θ values.

Spectra such as those in Fig. 2 will result if the spin labels all have the same orientation relative to the myosin heads, the heads all have the same orientation relative to the fiber axis (these two orientations determine θ'), and the fiber axes all have the same orientation (ψ) relative to the magnetic field. Heterogeneity in any of these orientations will broaden the EPR spectra. For example, if the fibers are all parallel to the field ($\psi = 0$ so $\theta = \theta'$) and the distribution of label orientations relative to the fiber axis is given by a spherically-weighted gaussian function:

$$\rho(\theta) = \sin\theta \exp\left[-\ln 2 \frac{\theta - \theta_0}{\Delta\theta}\right]^2, \tag{4}$$

then spectra like those in Fig. 3 will be observed. To a good approximation, θ_0 (the center of the gaussian angular distribution) determines the positions of the spectral lines, while $\Delta\theta$ (the full width at half maximum of the gaussian angular distribution) determines the line widths.

It is, in principle, possible to integrate the first derivative experimental spectrum, yielding the distribution function for H_{res} (θ, m_I), and then to use Eq. 2 to solve directly for the distribution function of $\cos^2\theta$. However, we have found it more convenient to determine the

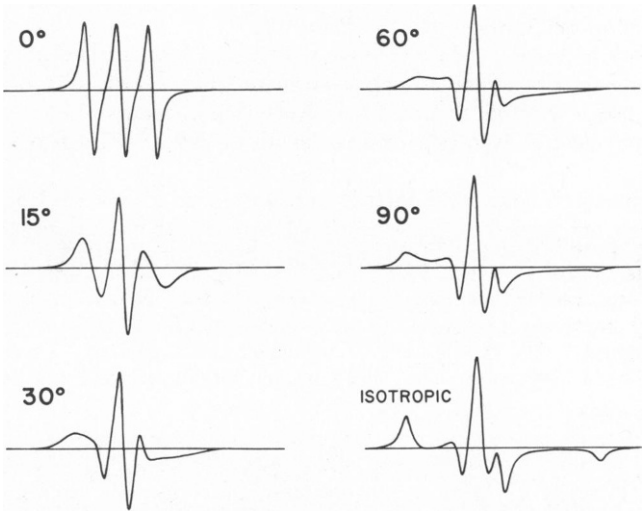

FIGURE 3 Simulated EPR spectra from spin labels having a spherically weighted gaussian distribution of orientations $\theta = \theta'$ relative to the magnetic field (fiberaxis), as given in Eq. 4. The center of the gaussian component of the distribution (θ_0) is fixed arbitrarily at 75°. Values of the angular spread $\Delta\theta$ (full width at half maximum of the gaussian component) are indicated. The spectrum labeled "isotropic" corresponds to the limit of large $\Delta\theta$ and is independent of θ_0. This is the spectrum of an isotropically oriented ("powder") ensemble of spin labels, and is like that reported for myosin heads in suspensions of myofibrils or actomyosin (Thomas et al., 1980).

angular distribution by fitting experimental spectra with simulated spectra such as those in Fig. 3. This results in no significant ambiguity, since the error limits can be reliably established by comparing each experimental spectrum with a series of simulated spectra. For example, if the angular distribution is approximately gaussian, it is usually possible to determine the center and width of $\rho(\theta)$ with uncertainties of one or two degrees.

EXPERIMENTAL METHODS

Small strips of rabbit psoas muscle (1–2 mm diam) were dissected and glycerinated as described by Cooke and Bialek (1979). Muscle strips were removed from the sticks on which they were glycerinated and dissected into bundles of ~25–50 fibers. These were washed in rigor solution (0.12 M KCl, 5 mM $MgCl_2$, 1 mM EGTA, and 20 mM TES, pH 7.0) at 0°C for 30 min. They were transferred to the labeling solution (rigor solution plus 1 mM pyrosphosphate [PP_i]). IASL (*N*-[1-oxyl-2,2,6,6-tetramethyl-4-piperidinyl] iodoacetamide, from SYVA Co., Palo Alto, Calif.) was added to a concentration of 10^{-4} M and removed after 1 h by washing the fibers in labeling solution, then with rigor solution. The fibers were then treated with 25 mM $K_3Fe(CN)_6$ in rigor solution without KCl for 2 h. This process rather selectively destroyed the signal from labels that were not rigidly attached to myosin heads (Thomas et al., 1980). The $K_3Fe(CN)_6$ was then removed by washing in rigor solution. The same procedure was used with MSL (*N*-[1-oxyl-2,2,6,6-tetramethyl-4-piperidinyl] maleimide, from SYVA Co.), except that the concentration of label was 5×10^{-5} M, the labeling time was 15 min, and the $K_3Fe(CN)_6$ treatment lasted 18–24 h at 50 mM.

Myosin was prepared by a modification of the method of Tonomura, Appel, and Morales (1966) as described by Crooks and Cooke (1977). S-1 was prepared by papain digestion of myofibrils as described by Cooke (1972) and HMM was prepared by chymotryptic digestion of myosin as described by Weeds and Taylor (1975). Myosin, HMM, and S-1 were labeled with IASL as described by Thomas et al. (1980). AMPPNP (β, γ-imido-ATP) was purchased from Sigma Chemical Co., St. Louis, Mo.

EPR experiments were performed on a Varian E4 spectrometer equipped with a variable temperature controller (Varian Associates, Instrument Div., Palo Alto, Calif.). Fibers were contained in a specially designed flat cell made of Kel-F, in which the fiber bundles, ~0.5 mm in diameter and 7 mm in length, were enclosed and oriented either parallel or perpendicular to the magnetic field. In some cases, the ends of the fibers were tied with surgical thread to prevent length changes. Lucite windows in the cell permitted the measurement of average sarcomere length by optical diffraction, using a helium-neon laser.

Tension measurements on actomyosin threads were performed as described by Crooks and Cooke (1977). Measurements on fibers were made as described by Bialek and Cooke (1979). Fiber bundles (2–5 fibers) were used and contraction was produced by addition of 5 mM ATP in the presence of 10^{-4} M free Ca^{2+}.

RESULTS

Spin Labeling

The methods used to spin-label fibers were essentially those used to label myofibrils (Thomas et al., 1980). In that study, labeling conditions (temperature, ionic strength, pyrophosphate), extent of labeling, and $K_3Fe(CN)_6$ treatment were adjusted to maximize the specificity of labeling myosin heads, resulting in spin labels rigidly attached to the heads (Thomas et al., 1980). In the resulting preparations, labeled either with IASL or MSL, at least 90% of the label is attached to myosin heads. In fact, as shown below, the high degree of orientation of these spin labels suggests that a specific group has been labeled. Based on the ATPase activities of extracted myosin at high ionic strength in the presence of EDTA, the reaction

appears to be selective for the SH-1 thiol groups (Thomas et al., 1980). The ATPase activity of myofibrils labeled by a similar procedure was nearly normal, and the actin-activated ATPase activity of myosin extracted after spin-labeling was not significantly affected by labeling (Thomas et al., 1980). The ratio of spin labels to heads was in the range of 0.2–0.4. At this level of labeling, specificity for myosin heads was maximized and fibers retained their ability to develop tension. At levels of labeling sufficient to label all the heads, labeling was no longer specific for the heads and tension was significantly inhibited.

When myosin, HMM, and S-1 were spin-labeled with IASL, the labels reacted selectively with the SH-1 thiol groups of myosin (Thomas et al., 1980). In contrast to the labeled fibers, however, the reaction was complete: there were 0.8–1.0 spin labels bound per myosin head. Actomyosin threads made from IASL myosin and unlabeled actin produced the same tension as controls, showing that a spin label on the SH-1 group of the myosin head does not impair its ability to produce isometric tension. Thus the decreased tension seen when fibers are extensively labeled probably is the result of labels on sites other than the SH-1 of the myosin head.

EPR Spectra

RIGOR Fig. 4 shows EPR spectra from spin-labeled fibers in rigor, with the fibers oriented parallel (solid curves) and perpendicular (dashed curves) to the magnetic field. The large differences between the solid and dashed curves indicate that the spin labels are highly ordered (have a narrow orientation distribution) relative to the field.

Fig. 5 again shows the spectra from fibers oriented parallel to the field, along with the best fits of Eq. 4 to the data. The fits are quite good, indicating that the gaussian distribution model is a useful one in describing these spectra. Although the two spin labels yield similar angular spreads ($\Delta\theta$ of 17° for IASL, 15° for MSL) the centers of the distributions are clearly different (θ_0 = 68° for IASL, 82° for MSL). The most likely explanation for this result is that the spread in angles is determined in both cases by the same narrow orientation distribution of the heads relative to the fiber axis, but the two labels bind at different angles relative to the heads. Thus the two probes, which are probably attached to the same SH group, apparently have their nitroxide groups in different environments. This is consistent with the observation that a conformational change in the head during ATPase activity is sensed by IASL but not by MSL (Thomas et al., 1980). Although the fits to the narrow gaussian distributions are remarkably good, there are small peaks at the low- and high-field regions corresponding to the spectrum of an isotropic distribution of probes (see Fig. 3, bottom right). Simulations indicate that, for both IASL and MSL, these unoriented components represent no more than 10–20% of the spin labels contributing to the spectrum. In some preparations of IASL-fibers, this component is <5% of the total.

To determine whether the observed orientation is controlled by the thick or thin filament lattice, we added spin-labeled S-1 and HMM to unlabeled fibers. Fiber bundles were incubated in a rigor solution containing ~10 mg/ml of IASL-S-1 or IASL-HMM, then washed with rigor solution to remove unbound fragments. Incubation longer than 30 min resulted in no further increase in the signal intensity from washed fibers, so a 30-min incubation was used to prepare the samples for Fig. 6, which show spectra obtained with the magnetic field parallel to the fibers. Note that the spectra from the labeled fragments bound to unlabeled fibers (bottom two spectra in Fig. 6) are virtually identical to those from labeled

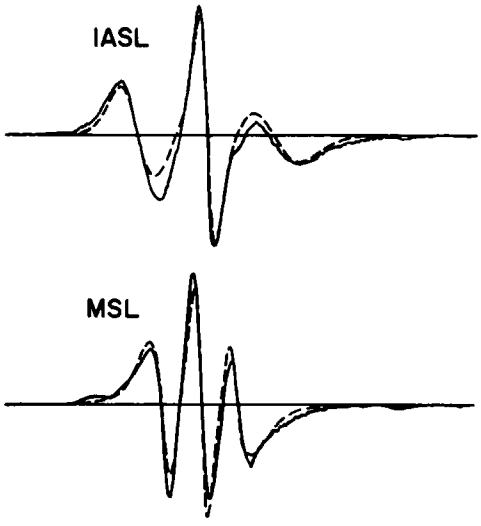

FIGURE 4

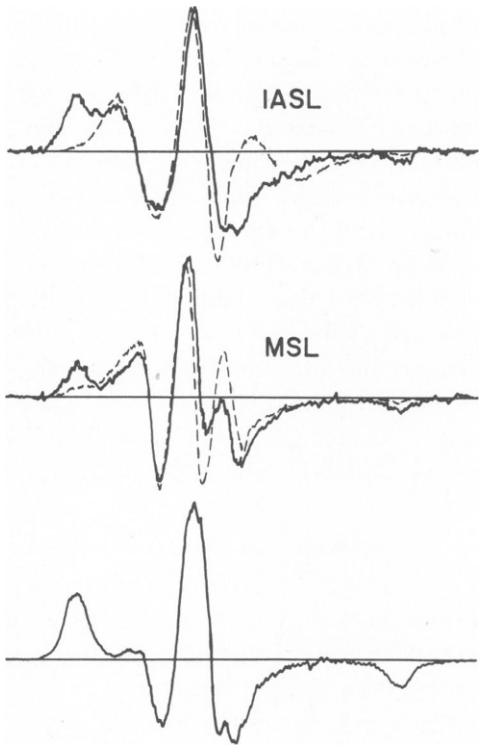

FIGURE 5

FIGURE 4 EPR spectra from spin-labeled fibers in rigor, with the fibers oriented parallel (solid curves) and perpendicular (dashed curves) to the magnetic field. The temperature was 20°C.

FIGURE 5 Comparison of experimental (solid curves, from Fig. 4) and simulated (dashed curves) EPR spectra for spin-labeled fibers in rigor, with the fibers oriented parallel to the magnetic field. The paramaeters used to produce the dashed curves are $\theta_0 = 68°$ and $\Delta\theta = 17°$ for IASL, $\theta_0 = 82°$ and $\Delta\theta = 15°$ for MSL. Where θ_0 is the center and $\Delta\theta$ is the full width at half maximum of the gaussian component of the distribution (see Eq. 4).

fibers (Fig. 6, top). Thus, it appears that the bond between actin and the myosin head determines the probe orientation.

Fig. 7 demonstrates further that the observed orientation is due to rigor bonds between myosin and actin. The top two spectra show the effects of stretching fibers from their rest length of 2.2 ± 0.1 μm/sarcomere (dashed curves) to a length of 3.2 ± 0.1 μm/sarcomere (solid curves). These effects are reversible: contracting the stretched IASL-fibers back to a 2.2-μm sarcomere length produces a spectrum like the dashed curve. The bottom spectrum was obtained after mincing MSL-fibers to randomize the fiber orientations. Note the similarity between this spectrum and the simulated spectrum corresponding to an isotropic orientation distribution (Fig. 3). Essentially the same spectrum is attained from minced IASL-fibers and from an actomyosin solution containing either MSL-myosin or IASL-myosin.

It appears that the spectra from stretched rigor fibers (Fig. 7, top two spectra, solid curves) can be resolved into two components, one corresponding to the highly oriented distribution of

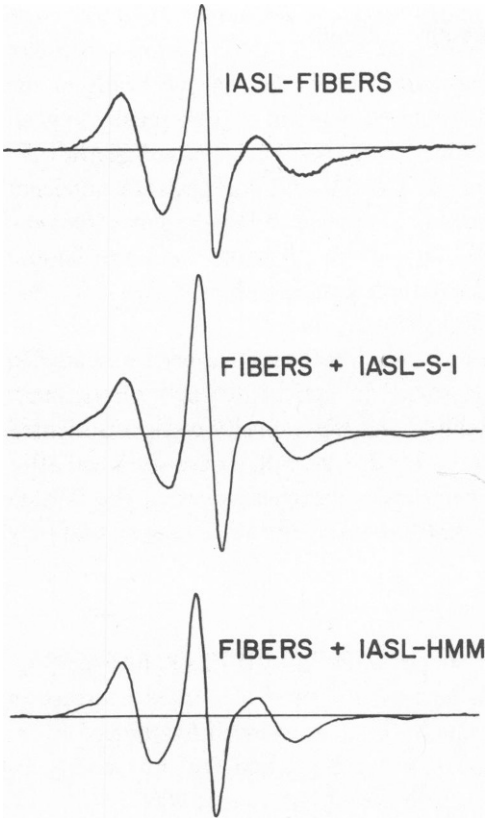

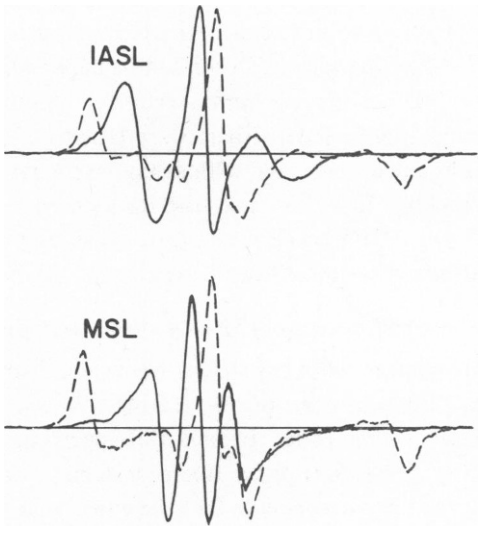

FIGURE 6

FIGURE 7

FIGURE 6 EPR spectra of unlabeled fibers decorated with spin-labeled myosin fragments at 20°. The fibers were oriented parallel to the magnetic field. (top) IASL-fibers, as in Figs. 4 and 5. (center) Unlabeled fibers decorated with IASL-S-1. (bottom) Unlabeled fibers decorated with IASL-HMM.

FIGURE 7 Effect of stretching on the EPR spectra of heads in fibers parallel to the magnetic field. Fibers were in rigor solution (0.12 M KCl, 5 mM $MgCl_2$, 1 mM EGTA, 20 mM TES, pH 7.0) at 20° during spectral recording. The top two spectra were obtained from oriented fibers at rest length (100% overlap, 2.2 ± 0.1 μm/sarcomere) and at a length corresponding to only 35–40% overlap (3.2 ± 0.3 μm/sarcomere). Each fiber bundle was tied at one end to the EPR cell with surgical thread, bathed in relaxing solution at 4°C, stretched, tied at the other end, and washed with rigor solution. The sarcomere lengths were measured in the EPR cell by optical diffraction. These lengths were the same before and after recording spectra. The diffraction pattern of the stretched fibers was distinct but more diffuse than that of unstretched fibers. The bottom spectrum was obtained from unstretched MSL-fibers in rigor, minced to randomize the orientations of the fibers.

unstretched fibers (Fig. 7, dashed curves), and another corresponding to an isotropic distribution (Fig. 7, bottom). In fact, the spectra from streched fibers can be simulated quite well by adding appropriate proportions of these two components. The best fits indicate that 31 ± 6% of the spin labels in the stretched IASL-fibers and 36 ± 8% of those in the stretched MSL-fibers have the orientation originally observed in unstretched fibers. It should be noted that the relative heights of two peaks do not necessarily correspond to the fractions of labels contributing to the two peaks; e.g., a given height for the low-field peak in the random

distribution represents approximately twice as many labels as the same height for the low-field peak in the well oriented distribution. Assuming that 2.2- and 3.8-μm sarcomere length correspond to 100% and 0% overlap, respectively, 37 ± 13% of the heads in the stretched preparations (sarcomere length, 3.2 μm) are in the filament overlap region, in good agreement with the percent of oriented heads determined from the EPR spectra. Spectra were recorded for IASL-fibers at several different sarcomere lengths, and the spectral component corresponding to an isotropic distribution increased with sarcomere length. For sarcomere lengths of 3.8 μm or more, the spectrum was nearly indistinguishable from the bottom spectrum in Fig. 7, corresponding to an isotropic distribution. Considerable disorientation was also observed in fibers contracted to lengths much less than 2.2 μm.

All of the spectra shown in this paper were obtained from fibers that had been spin-labeled at full overlap (2.2-μm sarcomere length, as measured by optical diffraction). In other experiments, IASL-fibers were labeled after stretching, and the intensity of the disoriented component increased with sarcomere length, just as in IASL-fibers that were stretched after labeling. In either case, the disoriented spectral component disappeared when the labeled fibers were allowed to shorten to rest length. Note that this rules out the possibility that only attached (oriented) heads react with the spin label.

Effects of ATP and ATP Analogues

By contrast with the sharp orientation distribution of spin labels in MSL-fibers in rigor (Fig. 8, top) the spectrum in relaxing solution (Fig. 8, bottom) indicates a marked decrease in orientational order. In fact, this spectrum is very much like that observed for minced fibers (Fig. 7, bottom) or for fibers stretched to zero overlap. Using Eq. 4 and Fig. 3 to model this spectrum, we conclude that the gaussian distribution width would be at least 90°.

When the unhydrolyzable ATP analog, AMPPNP, is added to fibers in rigor solution, the resulting spectrum is very similar to that observed for partially stretched MSL-fibers (Fig. 7, center). That is, it appears to have two components, one corresponding to the high degree of orientation observed in rigor (Fig. 8, top) and another corresponding to the nearly isotropic distribution observed in relaxing solution (Fig. 8, bottom), in minced myofibrils (Fig. 7, bottom), or in fibers stretched to zero overlap. When analyzed as a sum of rigor and isotropic spectra, the AMPPNP spectrum indicates that 37 ± 7% of the probes have the rigor orientation. Similarly, pyrophosphate (PP_i) produces a spectrum indicating that 27 ± 5% of the probes retain the rigor orientation, with the rest randomized as in relaxation. The effects shown in Fig. 8 are reversible. That is, when the ATP is completely hydrolyzed or when the AMPPNP or PP_i is washed out, the rigor spectrum is observed (Fig. 8, top). The "relaxed" spectrum (Fig. 8, bottom) was recorded before the return to rigor began.

DISCUSSION

The orientational resolution of the nitroxide EPR spectrum makes spin labels uniquely powerful in the study of molecular orientation in organized systems. The principal difficulty is in selectively spin-labeling a single class of sites. Accordingly, most previous studies of orientation with spin labels have involved the study of purified components that could be labeled and then allowed to self-assemble into an ordered system. Examples are studies of lipids in oriented bilayers (Gaffney and McConnell, 1974; Smith and Butler, 1976) and

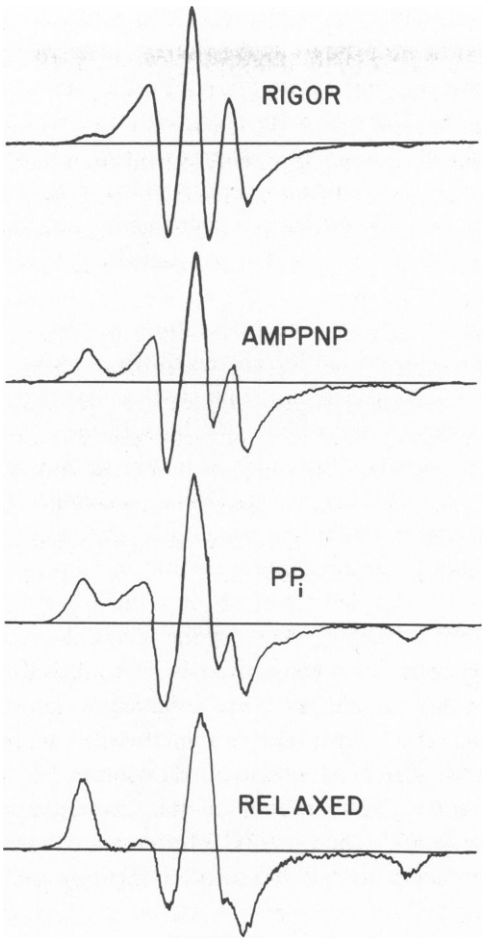

FIGURE 8 Effects of ATP and ATP analogues on orientation of spin-labels (MSL) on myosin heads at 0°C. The fibers were oriented parallel to the magnetic field. (*Rigor*) Same conditions as in Figs. 4–7. (*AMPPNP*) Fibers were soaked in rigor solution plus 1 mM AMPPNP. (PP_i) Fibers were soaked in rigor solution plus 1 mM PP_i.(*Relaxed*) Fibers were soaked in rigor solution plus 5 mM ATP, 15 mM creatine phosphate, and 0.5 mg creatine phosphokinase/ml.

proteins in single crystals (Chien, 1979; Bauer and Berliner, 1979). The present work establishes the utility of this approach in the study of intact multicomponent systems, in the case that a procedure can be developed for selectively labeling a single site.

Uniform Orientation of Myosin Heads in Rigor

The most striking property of probes attached to fibers in rigor at rest length is that, when the fibers are aligned parallel to the magnetic field, the spectra consist of sharp lines (Figs. 4 and 5) indicating that most of the probes have approximately the same orientation with respect to the fiber axis. For each probe there is a narrow distribution of orientations with a full width at half maximum of ~15°, strongly suggesting that the probe in each preparation is attached mainly to one class of sites, and that these sites are uniformly oriented relative to the fiber

axis. For both spin labels, these oriented probes are probably on the SH-1 thiol groups (Thomas et al., 1980). The narrow distribution of probe orientations indicates that the heads themselves have a narrow distribution of orientations relative to the fiber axis. Previous studies on myosin heads (S-1) labeled with IASL indicated that, if S-1 is assumed to be a prolate ellipsoid, the principal axis of IASL is approximately aligned with the long axis of S-1 (Thomas et al., 1975), so that the orientation distribution of heads should be similar to that observed for IASL. Thus, our best estimate is that the average angle between the head axis and the fiber axis (θ_0 in Eq. 4) is 68°, and that the full width of this orientation distribution is 17° or less.

The structural basis of the sharp head orientation in labeled fibers is indicated by the virtually identical orientation observed for unlabeled fibers irrigated with myosin fragments (S-1 and HMM, Fig. 6). Electron microscope studies have shown that S-1 diffuses into glycerinated fibers and binds to actin filaments, both in the *I* zone and in the zone where myosin and actin filaments overlap, forming a structure similar to that observed for F-actin decorated with S-1 in solution (Heuser and Cooke, unpublished observations). Thus, the orientation of the heads in rigor myofibrils is the same as that determined by the bond to actin, regardless of whether or not the heads are attached to the thick filament. It should be noted that 10–20% of the probes in labeled fibers are in a class having a random distribution of orientations, as determined from small peaks in the wings of the spectrum (Fig. 6, top). In principle, this leaves open the possibility that as many as 20% of the heads could be disoriented. However, the same small peaks are observed in the wings of the spectrum from unlabeled fibers (from the same preparation as the labeled fibers) irrigated with labeled S-1 or HMM (Fig. 6), suggesting that the observed disorientation is not due to the presence of detached heads, but to either disorientation of the filament axes or to probes that are disoriented relative to the head. In fact, in several preparations of IASL-fibers, the peaks in the wings of the spectrum were not present at all, indicating that no more than 5% of the probes were disoriented.

The above argument demonstrates that attachment of heads to actin is sufficient to produce the orientation observed in rigor fibers. That attachment is also necessary for orientation is demonstrated by the experiments on stretched fibers (Fig. 7) and relaxed fibers (Fig. 8) which show that eliminating the myosin-actin interaction produces a broad angular distribution of probes. Therefore, any unattached heads in rigor at full overlap would be expected to produce randomly oriented spectral components (peaks in the wings of the spectra) in excess of those observed for labeled S-1 or HMM bound to filaments. Since this is not observed, we conclude that virtually all of the myosin heads in a rigor fiber are attached to actin at full overlap, all at nearly the same orientation relative to the fiber axis. This conclusion is strongly supported by studies on the rotational motion of spin-labeled heads (Thomas et al., 1980), involving saturation transfer spectroscopy. That work showed that all (>90%) probes on heads in a rigor myofibril are immobilized on the submillisecond time scale, as observed for S-1 attached to F-actin, but that rapid rotational mobility is observed in relaxed myofibrils and synthetic myosin filatments.

Two important qualifications must be appended to this conclusion that all heads are attached in rigor. First, it is possible that only a single head of each pair is attached to actin, with the other being oriented due to interaction with its partner. Second, the sharp orientation

distribution applies only to that region of the head where the spin label is attached. It remains possible that some other region, presumably farther from actin, is less ordered.

Orientational Disorder of Heads Detached from Actin

The most straightforward interpretation of the results for relaxed or stretched myofibrils, showing a wide range (>90°) of probe orientations relative to the fiber axis, is that, in the absence of a bond with actin, the myosin head is free to assume a wide range of orientations. It is important to determine whether the observed disorientation reflects directly the behavior of the head or that of the probe relative to the head. The studies by Thomas et al. (1980) on spin-labeled myofibrils indicate that the source of this disorientation is rotational mobility on the time scale of ~10 μs. In that work, this rotational mobility was observed in synthetic myosin filaments (in the presence or absence of ATP) and in myofibrils in the presence of ATP, but not in myofibrils in rigor nor in isolated S-1 immobilized on glass beads (in the presence or absence of ATP). Therefore, the disorientation observed in stretched or relaxed fibers is probably due to large-amplitude submillisecond rotations, and this motion is probably that of the heads themselves. However, in the absence of direct measurements on rotational motion in fibers (in progress), we cannot rigorously rule out the possibility that some of the observed disorientation in stretched or relaxed fibers is due to static disorder, either of the heads themselves or of probes relative to the heads.

The simplest interpretation of the data is that we are observing large fluctuations in the angle θ (see Fig. 2) that a long rigid myosin head makes with the fiber axis. In the absence of precise knowledge of the shape and rigidity of the head and the orientation of the probe on the head, it should be noted that other kinds of rotations could be contributing to the observed disorder.

Our results indicate that the ATP analogs, AMPPNP and PP_i, produce states in which some of the probes have the same orientation as in rigor and the rest have the random orientation distribution observed in relaxation. These two populations may be in equilibrium with each other, but exchange between the two states must be on the microsecond time scale or slower. No significant fraction of the probes have shifted to another well-defined orientation. One interpretation of our results is that both AMPPNP and PP_i substantially decrease the fraction of attached crossbridges. Alternatively, a portion of the heads could be attached but disoriented.

In summary, the present EPR results, along with those of Thomas et al. (1980), suggest a simple two-state model for the orientational and rotational behavior of myosin heads. When the rigor interaction between myosin and actin is possible, i.e., when myosin heads are in the overlap zone and no nucleotides are present, heads are attached to actin, immobile, and uniformly oriented. When the myosin-actin interaction is eliminated by stretching or disrupted by ATP, unattached heads rotate freely through large angles in the submillisecond time range.

Relation to Other Work

In addition to the present EPR study, a number of methods have been used to obtain information on the orientation of myosin crossbridges in muscle fibers, although none of those methods can provide the direct and detailed information that is possible with EPR.

We conclude that in rigor fibers the myosin heads have a high degree of orientation. The polarization of fluorescent dyes attached to heads in glycerinated fibers (Nihei et al, 1974; Tregear and Mendelson, 1975; Borejdo and Putnam, 1977) also indicates that the dyes have a high degree of orientation. Electron micrographs of rigor insect flight muscle also show all attached bridges to have similar configurations (Reedy, 1967). We further conclude that virtually all heads are attached to actin in the rigor fiber. This conclusion is supported by the work of Cooke and Franks (1980) who used an enzymatic technique to estimate that no more than 5% of the heads in a rigorlike rabbit psoas fiber do not interact with actin. Quite different conclusions have been obtained from models of the structure of insect flight muscle based on electron microscope (EM) and x-ray diffraction data. These models have suggested that only one-third to three-quarters of the heads would bind to actin (Haselgrove and Reedy, 1978; Elliot and Offer, 1978; Holmes et al., 1980). This conflict could be due to a difference between insect and rabbit muscle; future EPR experiments on insect muscle should help settle the question. The present result, that heads in vertebrate striated muscle in rigor are not only attached to actin but also uniformly oriented by the actin helix, suggests that considerable flexibility must be present in the myosin structure, possibly in the portion of the crossbridge that connects the head to the filament core.

We conclude that the heads have a large amount of rotational disorder in relaxed fibers. The polarization of fluorescent dyes attached to the myosin heads also indicates a large amount of disorder, in qualitative agreement with our conclusion (Borejdo and Putnam, 1977). In contrast, the sharp layer lines seen in x-ray diffraction experiments on relaxed fibers in frog (Huxley and Brown, 1967; Haselgrove, 1975), rabbit (Rome, 1972; Lymn, 1975), and insect (Miller and Tregear, 1972) have led to models in which the myosin heads are well oriented at an angle of ~90° relative to the fiber axis. However, the present suggestion of rotational disorder is not necessarily in conflict with the diffraction data. It is difficult to predict precisely the effects of rotational disorder on the x-ray diffraction data. A first approximation to this calculation can be made by applying formulas derived to describe thermal fluctuations in crystals (Vainshtein, 1966). According to this analysis a root-mean-square fluctuation $\triangle$ in the axial position of the scattering mass will decrease the intensity of reflections by a factor $\exp(-19\,\triangle^2 S^2)$, where S is the magnitude of the scattering vector. We assume that the myosin head is tethered to a fixed lattice point (e.g., at the junction between S-1 and S-2). For a given angular fluctuation of the head, a point near the tether point will cause a smaller translational fluctuation $\triangle$ than a more distant point. The analysis indicates that large angular fluctuations (on the order of $\pm 45°$) relative to the fiber axis should decrease the intensity of the higher order reflections, but myosin layer lines out to the sixth order should still be visible, consistent with the x-ray data (Rome, 1972). Thus the x-ray diffraction data do not require sharp head orientation in relaxation, and the EPR results, which provide direct information about orientation, indicate that the previous picture of perpendicular crossbridges in relaxation is unlikely to be correct. It should be noted that the material used in the present study, glycerinated rabbit psoas muscle, yields less intense x-ray diffraction patterns than does living resting frog muscle (Rome, 1972; Huxley and Brown, 1967), indicating that the latter system is better ordered. Therefore, coordinated EPR and x-ray measurements on the same preparation would be very interesting.

X-ray diffraction data on glycerinated fibers, both rabbit psoas (Lymn, 1975) and insect

flight (Marston et al, 1976), suggest that AMPPNP changes rigor crossbridges toward the relaxed state. The present EPR results are consistent with such a model, and indicate that AMPPNP produces an orientation distribution that would be expected for a sum of the rigor and relaxed orientation distributions, and not a new orientational state intermediate between the two. As discussed above, there seem to be two likely interpretations of the present EPR data on AMPPNP effects: either a portion of the heads become disoriented due to detachment, or they assume a wide range of attached angles. Fiber stiffness, a mechanical property thought to indicate the fraction of attached crossbridges, is not greatly affected in either rabbit psoas or insect flight muscle (Marston et al., 1976) supporting the model that most of the crossbridges remain attached. Ishiwata, Seidel, and Gergely (private communication) have shown that submillisecond rotational mobility (measured by saturation transfer EPR) appears to be a reliable indicator of crossbridge detachment, and that AMPPNP induces rotational mobility under some conditions in rabbit myofibrils, supporting the model that crossbridges do become detached. A more definitive test of this model will require measurements of mobility (using saturation transfer EPR) and orientation (using conventional EPR) on the same fiber preparation.

The consequences of the EPR results for the mechanism of force generation must be clarified by future EPR experiments on Ca^{2+}-activated fibers. However, the present results suggest that considerable rotational freedom of heads may be present in the detached phase of the crossbridge cycle. Heads may be constantly undergoing spontaneous Brownian rotation through large angles. Instead of controlling precisely the orientation of the heads, the ATPase cycle may simply serve the purpose of regulating protein binding affinities so that the Brownian rotations are coupled vectorially to force generation.

We thank J. Gergely, J. C. Seidel, R. A. Mendelson, and R. T. Tregear for helpful discussions. We thank K. Franks and V. A. Barnett for technical assistance.

This work was supported by grants from the National Institutes of Health, National Science Foundation (PCM 80-04512), Muscular Dystrophy Association, and the Minnesota Medical Foundation.

Received for publication 11 June 1980 and in revised form 13 August 1980.

REFERENCES

ARONSON, J. F., and M. F. MORALES. 1969. Polarization of tryptophan fluorescence in muscle. *Biochemistry.* **8**:4517–4522.

BOREDO, J., and S. PUTNAM. 1977. Polarization of fluorescence from single skinned glycerinated rabbit psoas fibers in rigor and relaxation. *Biochim. Biophys. Acta.* **459**:578–595.

COOKE, R. 1972. A new method for preparing myosin subfragment-1. *Biochem. Biophys. Res. Commun.* **49**:1021–1028.

COOKE, R., and K FRANKS. 1980. All myosin heads form bonds with actin in rigor rabbit skeletal muscle. *Biochemistry.* In press.

CROOKS, R., and COOKE. 1977. Tension generated by threads of contractile proteins. *J. Gen. Physiol.* **69**:37–55.

DOS REMEDIOS, C. G., R. G. C. MILLIKAN, and M. F. MORALES. 1972. Polarization of tryptophan fluorescence from single striated muscle fibers. *J. Gen. Physiol.* **59**:103–120.

COOKE, R., and W. BIALEK. 1979. Contraction of glycerinated muscle fibers as a function of the ATP concentration. *Biophys. J.* **28**:241–258.

GAFFNEY, B. J., and H. M. MCCONNELL. 1974. The paramagnetic resonance spectra of spin labels in phospholipid membranes. *J. Magn. Reson.* **16**:1–28.

HASELGROVE, J. C. 1975. X-ray evidence for conformation changes in the myosin filaments of vertebrate striated muscle. *J. Mol. Biol.* **92**:113–143.

HASELGROVE, J. C., and M. K. REEDY. 1978. Modeling rigor cross-bridge patterns in muscle. *Biophys. J.* **24**:713–728.

HIGHSMITH, S., K. AKASAKA, M. KONRAD, R. GOODY, K. HOLMES, N. WADE-JARDETSKY, and O. JARDETSKY. 1979. Internal motions in myosin. *Biochemistry.* **18**:4238–4244.

HOLMES, K. C., R. T. TREGEAR, and J. BARRINGTON LEIGH. 1980. Interpretation of the low angle X-ray diffraction from insect flight muscle in rigor. *Proc. R. Soc. Lond. B Biol. Sci.* **207**:13–33.

HUXLEY, A. F., and R. M. SIMMONS. 1971. Proposed mechanism of force generation in stricted muscle. *Nature (Lond.).* **233**:533–538.

HUXLEY, H. E. 1969. The mechanism of muscular contraction. *Science (Wash. D.C.).* **114**:1356–1366.

HUXLEY, H. E., and W. BROWN. 1967. The low-angle X-ray diagram of vertebrate striated muscle and its behavior during contraction and rigor. *J. Mol. Biol.* **30**:383–434.

LYMN, R. 1975. Low-angle X-ray diagrams from skeletal muscle: the effect of AMP-PNP, non-hydrolyzed analogue of ATP. *J. Mol. Biol.* **94**:567–582.

LYMN, R., and H. E. HUXLEY, 1973. X-ray diagrams from skeletal muscle in the presence of ATP analogs. *Cold Spring Harabor Symp. Quant. Biol.* **37**:449–454.

MCCALLEY, R. C., E. J. SHIMSHICK, and H. M. MCCONNELL. 1972. The effect of slow rotational motion on paramagnetic resonance spectra. *Chem. Phys. Lett.* **13**:115–119.

MARSTON, S. B., C. D. RODGER, and R. T. TREGEAR. 1976. Changes in muscle crossbridges when β, -imido ATP binds to myosin. *J. Mol. Biol.* **104**:263–276.

MENDELSON, R. A., M. F. MORALES, and J. BOTTS. 1973. Segmental flexibility of the S-1 moiety of myosin. *Biochemistry.* **12**:2250–2255.

MENDELSON, R. A., S. PUTNAM, and M. MORALES. 1975. Time-dependent fluorescence depolarization and lifetime studies of myosin subfragment-one in the presence of nucleotide and actin. *J. Supramol. Struct.* **3**:162–168.

MILLER, A., and R. T. TREGEAR. 1972. Structure of insect fibrillar flight muscle in the presence and absence of ATP. *J. Mol. Biol.* **70**:85–104.

NIHEI, T., R. A. MENDELSON, and J. BOTTS. 1974. Use of fluorescence polarization to observe changes in attitude of S-1 moieties in muscle fibers. *Biophys. J.* **14**:236–242.

OFFER, G., and A. ELLIOT. 1978. Can a myosin molecule bind two actin filaments? *Nature (Lond.).* **271**:325–329.

REEDY, M. K. 1967. Crossbridges and periods in insect flight muscle. *Am. Zool.* **7**:465–481.

REEDY, M. K., K. C. HOLMES, and R. T. TREGEAR. 1965. Induced changes in orientation of the crossbridges of glycerinated insect flight muscle. *Nature (Lond.).* **207**:1276–1280.

ROME, E. 1972. Relaxation of glycerinated muscle: low-angle X-ray diffraction studies. *J. Mol. Biol.* **65**:331–343.

SMITH, I. C. P., and K. W. BUTLER. 1976. Oriented lipid systems as model membranes. *In* Spin Labeling. L. J. Berliner, editor. Academic Press, Inc., New York. 411–451.

THOMAS, D. D., J. C. SEIDEL, J. S. HYDE, and J. GERGELY. 1975 a. Motion of subfragment-1 in myosin and its supramolecular complexes: saturation transfer electron paramagnetic resonance. *Proc. Natl. Acad. Sci. U.S.A.* **72**:1729–1733.

THOMAS, D. D., L. R. DALTON, and J. S. HYDE. 1976. Rotational diffusion studied by passage saturation transfer electron paramagnetic resonance. *J. Chem. Phys.* **65**:3006–3024.

THOMAS, D. D., S. ISHIWATA, J. C. SEIDEL, and J. GERGELY. 1980. Submillisecond rotational dynamics of spin-labeled crossbridges in myofibrils. *Biophys. J.* **32**:873–890.

TONOMURA, Y., P. APEL, and M. F. MORALES. 1966. On the molecular weight of myosin. II. *Biochemistry.* **5**:515–521.

TREGEAR, R. T., and R. A. MENDELSON. 1975. Polarization from a helix of fluorophores and its relation to that obtained from muscle. *Biophys. J.* **15**:455–467.

TREGEAR, R. T., and S. B. MARSTON. 1979. The crossbridge theory. *Ann. Rev. Physiol.* **41**:723–736.

VAINSHTEIN, B. K. 1966. *Diffraction of X-rays by Chain Molecules.* Elsevier/North-Holland, New York.

WEEDS, A. G., and R. S. TAYLOR. 1975. Separation of subfragment-1 isoenzymes from rabbit skeletal muscle myosin. *Nature (Lond.).* **257**:54–56.

YOUNT, R. G., D. OJALA, and D. BABCOCK. 1971. Interaction of PNP and PCP analogues of adenosine triphosphate with heavy meromyosin, myosin, and actomyosin. *Biochemistry.* **2490–2495.**